Novel Compact Elliptic-Function Narrow-Band Bandpass Filters Using Microstrip Open-Loop Resonators With Coupled and Crossing Lines

Cheng-Cheh Yu, *Member, IEEE,* Kai Chang, *Fellow, IEEE*

***Abstract*— Novel compact elliptic-function narrow-band bandpass filters have been designed and fabricated. This new configuration consists of two identical microstrip open-loop resonators with coupled and crossing lines. A theoretical investigation has confirmed that this novel configuration is capable of providing elliptic-function filtering. Furthermore, the feasibility of this filter is verified experimentally. Centered at 2.039 GHz, the fabricated microstrip bandpass filter shows a measured 3-dB bandwidth of 2% and two deep notches in its stopband. In addition, the main circuit of this filter occupies only 2.5 cm $\times$ 1.5 cm using a substrate with dielectric constant of 10.5, making it very attractive for applications in the mobile and personal communication systems (PCS's).**

***Index Terms*— Bandpass filters, elliptic-function filtering, microstrip resonator, narrow-band, personal communication systems.**

I. Introduction

HIGHLY desirable for modern mobile and personal communication systems (PCS's) are miniature high-performance narrow-band (1%–3%) bandpass filters having low insertion loss and sharp selectivity in the passbands. Planar filters are usually preferred whenever they are available and suitable because of their small sizes and low fabrication cost. Design techniques for conventional microstrip filters have long been well established [1]–[3]. However, these filters often suffer from impracticality for passbands of less than 5%.

Recently, a class of dual-mode microstrip filters using microstrip ring resonators was devised, which makes the realization of narrow-band elliptic-function designs in a planar configuration [4]–[8] practical. Inspection of the end-coupled dual-mode ring filters in [4] and [5] shows that the insertion loss obtained is around 4 dB. In order to reduce the transmission loss, tapped lines are used in [6]–[8] to enhance the coupling strength at the input and output terminals. From their measured results, the insertion loss has been improved to about 2 dB. However, the measured 3-dB bandwidth has also been increased to a value around 4%, as shown in their experimental results. Although the insertion loss due to insufficient coupling strength can be improved by increasing the coupling region, the attenuation due to conductor and dielectric losses may only be reduced by high-temperature superconducting thin-film technology [9]–[11] or by combining with active devices to compensate them [12]. In [13], a new microstrip elliptic-function narrow-band bandpass filter is proposed. This configuration is quite compact in size, yet a measured 3-dB bandwidth of 4% was reported for a four-pole filter.

In this paper, novel compact elliptic-function narrow-band bandpass filters using microstrip open-loop resonators with coupled and crossing lines have been developed. The 3-dB bandwidth of this novel filter centered at 2.039 GHz is measured about 2%, and its main circuit size occupies only 2.5 cm $\times$ 1.5 cm. For convenience of subsequent understanding and comparison, the theoretical and experimental frequency responses of a two-section coupled ring filter is given in Section II. Then, a novel compact bandpass filter using open-loop resonators and coupled lines, which showed a narrower 3-dB bandwidth than the coupled ring filter, was introduced and implemented in Section III. By adding a crossing line to the preceding filter, both the simulated and measured performances in Section IV proved that another new compact configuration of elliptic-function narrow-band bandpass filter could thus be formed. All the aforementioned filters were fabricated on an RT/Duroid 6010.5 substrate with a dielectric constant of 10.5, substrate thickness of 50 mil, and conductor thickness of 1.4 mil. In addition, 50-Ω lines of width $W_r = 1.145$ mm were used for all the connecting lines constituting these filters. Finally, an HP 8510B automatic network analyzer was used to accurately measure their transmission performances.

II. Frequency Responses of a Coupled Ring Filter

A. A Two-Section Ring Filter End Coupled to Input/Output Lines Directly

A two-stage conventional microstrip bandpass filter that uses half-wave resonators is shown in Fig. 1, where single resonator length = 30.5 mm, input/output coupling gap sizes $S_1 = S_2 = 0.1$ mm, and interstage coupling gap size $S_{12} = 1.5$ mm. On the other hand, Fig. 2 illustrates the structure of a two-stage coupled square ring filter in which single ring circumference = 63.8 mm, input/output gaps $S_1 = S_2 = 0.1$ mm, and interstage gap $S_{12} = 2.2$ mm. Using the widely used EEsof Touchstone software[1] for transmission-line

Manuscript received May 27, 1997; revised April 7, 1998.

C.-C. Yu is with the National Taipei University of Technology, Taipei, Taiwan 10643, R.O.C.

K. Chang is with the Department of Electrical Engineering, Texas A&M University College Station, TX (e-mail: chang@eesun1.tamu.edu).

Publisher Item Identifier S 0018-9480(98)04956-4.

[1] *Touchstone,* EEsof, Inc., Westlake Village, CA, 1993.

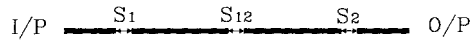

Fig. 1. Schematic diagram of a two-section end-coupled half-wave microstrip bandpass filter.

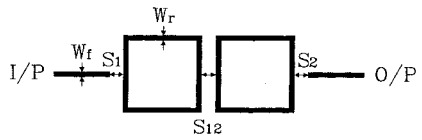

Fig. 2. Arrangement of a two-section microstrip ring filter directly coupled to input/output lines.

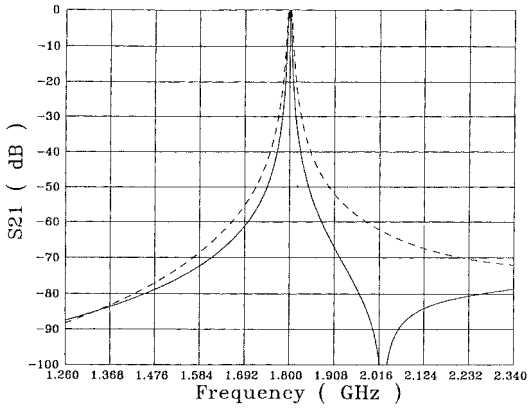

Fig. 3. Comparison of the theoretical frequency responses of the conventional resonator filter in Fig. 1 (dashed line) and the coupled ring filter in Fig. 2 (solid line).

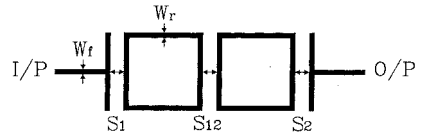

Fig. 4. Layout of a two-section ring filter edge coupled to tapped input/output lines.

circuit analysis, both the theoretical frequency responses of the two microstrip bandpass filters are given in Fig. 3.

As can be obviously seen in Fig. 3, the ring resonator filter presents an attenuation notch in the upper stopband and has steeper attenuation slopes, as compared to the conventional capacitively coupled half-wave resonator filter. This makes it clear that the ring filter is able to provide narrower bandwidth in the passband and better rejection in the stopband. Although, by changing the feed line positions and the coupling length between the ring resonators adequately, another notch may be created in the lower stopband to provide further improvement, insertion losses of up to 8 dB are quite typical for actual end-coupled ring filters [14], [15].

B. A Two-Section Ring Filter Edge Coupled to Tapped Input/Output Lines

In order to improve the insertion loss of the coupled square ring filter, the tapped input/output lines, shown in Fig. 4, are utilized to increase the coupling region. The parameters used in this configuration are as follows: ring linewidth $W_r = W_f = 1.145$ mm, mean loop periphery $= 63.8$ mm, $S_1 = S_2 = 0.4$ mm, and $S_{12} = 1.5$ mm. Both the computer simulation and measured results are provided in Fig. 5. The experimental results are shown to be in reasonable agreement with the theoretical frequency responses. Centered at 1.760 GHz, the actual insertion loss and 3-dB bandwidth are measured as 2.3 dB and 3.7%, respectively. Additionally, there is a notch in the upper stopband, which is not displayed in this figure since its position is beyond the given range.

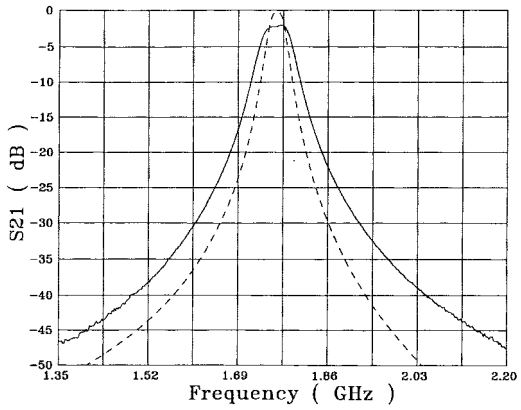

Fig. 5. Theoretical (dashed line) and measured (solid line) frequency responses of the coupled ring filter of Fig. 4.

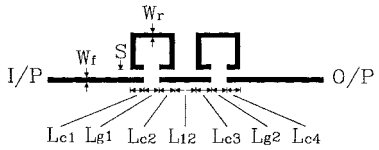

Fig. 6. A novel compact bandpass filter using open-loop resonators and coupled lines.

In view of Sections II-A and II-B, it is evident that the ring filter can offer a narrower passband bandwidth and sharper stopband rejection than the conventional end-coupled resonator filter, but strong coupling enhancement is usually needed to improve its insertion loss to an acceptable level. In the following section, a novel bandpass filter using open-loop resonators and coupled lines will be presented. It will be shown that this novel filter is relatively compact in size and capable of providing a narrower bandwidth than the coupled ring filter just described.

III. A Novel Bandpass Filter Using Open-Loop Resonators and Coupled Lines

A. Coupling Enhancement by Edge-Coupled Lines

As demonstrated in Section II, end-coupled filters usually suffer insufficient coupling strength while edge-coupled structures are able to give acceptable passband insertion loss. In view of this observation, the new configuration, as shown in Fig. 6, is devised. This novel compact bandpass filter consists of two identical open-loop resonators and coupled lines, which are adequately adjusted to obtain sufficient coupling gap capacitance. In order to have a reasonable estimation of the coupling gap capacitance between short sections of coupled microstrip lines, it may be approximated by that between two

symmetric coplanar strips (CPS's) with infinite thick substrate [16]. The capacitances contributed by the electric fields in the air and dielectric regions, respectively, are given by

$$C_{\text{air}} = \varepsilon_0 \frac{K'(m)}{K(m)} (F/m) \tag{1}$$

$$C_{\text{dielectric}} = \varepsilon_0 \varepsilon_r \frac{K'(m)}{K(m)} (F/m) \tag{2}$$

where $K(m)$ and $K'(m)$ are the complete elliptic integrals of the first kind and its complement [17] with argument $m = \sqrt{(\text{CPS gap size})/(2 \times \text{CPS linewidth} + \text{CPS gap size})} = \sqrt{S/(2 \times W_{\text{CPS}} + S)}$. For convenience of reference, these are explicitly given below:

$$K(m) = \int_0^{\pi/2} \frac{d\theta}{\sqrt{1 - m \sin^2 \theta}} \tag{3}$$

$$K'(m) = K(1 - m). \tag{4}$$

With the aids of (1)–(4), the total capacitance C_{total} for a coupling length L_{CPS} becomes

$$C_{\text{total}} = \varepsilon_0 (1 + \varepsilon_r) \frac{K'(m)}{K(m)} L_{\text{CPS}}(F). \tag{5}$$

For evaluation of the gap capacitance between the end-coupled microstrip lines in Fig. 1 with linewidth $W_f = 1.145$ mm, gap size $S = 0.1$ mm, and $\varepsilon_r = 10.5$, the formulas derived by Garg and Bahl [18] can be applied to calculate microstrip gap capacitance or the structure in the vicinity of the gap and may be viewed as a short CPS line with $L_{\text{CPS}} = W_f$ and $W_{\text{CPS}} = 50S$ as long as the coupling gap is the main concern. Using (1)–(5), the total coupling capacitance was found to be 0.186 pF. Moreover, it has also been noted that no noticeable capacitance was observed when W_{CPS} was increased further from $50S$ to $100S$, trying to obtain better approximation for the coupling gap between the end-coupled lines. On the other hand, the coupling gap between edge-coupled transmission lines in Fig. 6 with linewidth $W_f = 1.145$ mm, gap size $S = 0.15$ mm, coupling length $L_c = 2.5 \times W_f$, and $\varepsilon_r = 10.5$ can be well approximated by that of a CPS line with $W_{\text{CPS}} = W_f$ and $L_{\text{CPS}} = L_c$. After substituting these parameters into the above equations, the total coupling capacitance between the two edge-coupled lines was calculated to be 0.372 pF, which is two times the capacitance for the previous end-coupled lines.

From the aforementioned examples, it is clear that a small section of edge-coupled lines can provide more coupling strength and adjustment flexibility than the end coupled ones.

B. Design Considerations

The main considerations in the design of it are stated below.

1) The open-loop resonator length is set to approximately a half wavelength at the frequency of interest.
2) The two ends of each open-loop resonator are placed sufficiently apart in order to prevent unnecessary self end coupling.
3) For a given coupling gap size, the lengths of the input and output coupled lines are adjusted to obtain enough coupling strength at the operating frequency.

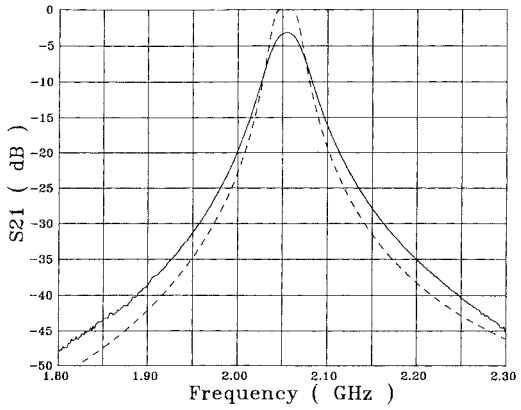

Fig. 7. Theoretical (dashed line) and measured (solid line) frequency responses of the novel compact filter, as depicted in Fig. 6.

4) A short auxiliary open-ended stub is used to edge couple the signal between the two open-loop resonators. The portions coupled along the ends of the resonators are tuned to meet the bandwidth requirement.
5) The length of the preceding auxiliary coupling stub should be long enough to keep the sides of the two open-loop resonators from being directly coupled to each other. On the other hand it is made as short as possible in order to keep the circuit compact.

C. Theoretical Result and Experimental Performance

Based on the above description, an experimental filter was designed and implemented. The parameters designated in Fig. 6 are as follows: open-loop resonator length = 27.61 mm, $S = 0.15$ mm, $L_{c1} = L_{c4} = 2.90$ mm, $L_{c2} = L_{c3} = 3.29$ mm, $W_r = W_f = 1.145$ mm, $L_{g1} = L_{g2} = 3W_f$, and $L_{12} = 4W_f$.

As shown in Fig. 7, the measured transmission characteristics are found to be in good agreement with the theoretical frequency response obtained by EEsof software. Moreover, the insertion loss and 3-dB bandwidth centered at 2.056 GHz are measured as 3.1 dB and 1.8%, respectively. Compared to the performance of the coupled ring filter, which shows a 3-dB bandwidth of 3.7% in Section II-B, this new bandpass filter is able to give much narrower 3-dB bandwidth. In addition, the circuit size is smaller (2.5 × 1 cm as compared to the 3 × 1.5 cm for the coupled ring filter) and can be further reduced if substrates with higher dielectric constants are used. Since bandpass filters with less than 2% bandwidth are usually needed for the mobile and PCS's, this novel compact filter may serve as a promising candidate.

Although 3.1-dB insertion loss is quite typical for laboratory prototype filters, it can be further improved by adhering dielectric overlays over the coupling gaps [19], [20]. Placing two 2 mm × 2 mm dielectric overlays with dielectric constant = 10.5 and thickness = 50 mil on both the interstage coupling gaps, the measured frequency responses are shown in Fig. 8, together with the results without the dielectric overlays. As can be clearly seen, the insertion loss has been decreased from 3.1 to 2.5 dB. Although the 3-dB bandwidth has also been increased from 1.8% centered at 2.056 GHz to 2.8% centered at 2.026 GHz, it is still narrower than that of the coupled ring filter.

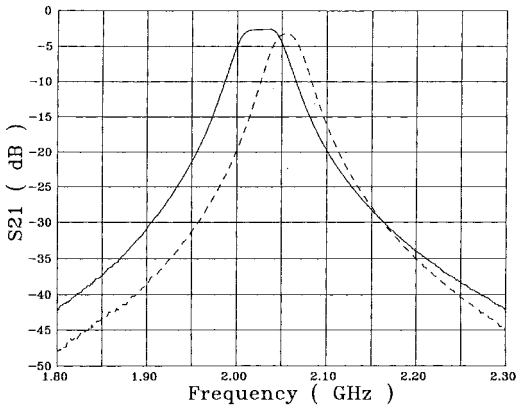

Fig. 8. Comparison of the measured frequency responses of the novel filter in Fig. 6 with (solid line) and without (dashed line) dielectric overlays of relative dielectric constant = 10.5 and thickness = 50 mil placed on both the interstage coupling gaps.

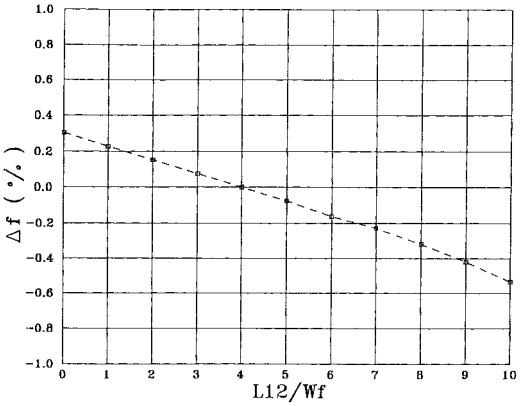

Fig. 9. Simulated percentage center-frequency drift $\Delta f = [f_0(L_{12}) - f_0(L_{12} = 4W_f)]/f_0(L_{12} = 4W_f) \times 100\%$ versus the interstage coupling stub length L_{12}, as indicated in Fig. 6.

D. Effects of the Interstage Coupling Stub on Center Frequency and Bandwidth

As mentioned previously, a short auxiliary open-ended stub is used to provide the interstage coupling and keep the open-loop resonators from being coupled to each other directly. It is necessary to have a clear understanding about the influence of its noncoupled length upon the center frequency and 3-dB bandwidth of the filter being considered. Letting the center frequency f_0 with $L_{12} = 4W_f$ be the reference value, the center frequency drift Δf is defined as

$$\Delta f = [f_0(L_{12}) - f_0(L_{12} = 4W_f)]/f_0(L_{12} = 4W_f) \times 100\%. \tag{6}$$

Using EEsof software, the effects of the noncoupled section of the auxiliary coupling stub L_{12}, as indicated in Fig. 6, have been investigated. Displayed in Fig. 9 is the simulated percentage center-frequency drift Δf versus L_{12}/W_f, and the simulated variations of the percentage 3-dB bandwidth with L_{12}/W_f are given in Fig. 10. According to the results obtained, both the frequency drift and the bandwidth change are within 0.5% for practical interstage coupling stub lengths.

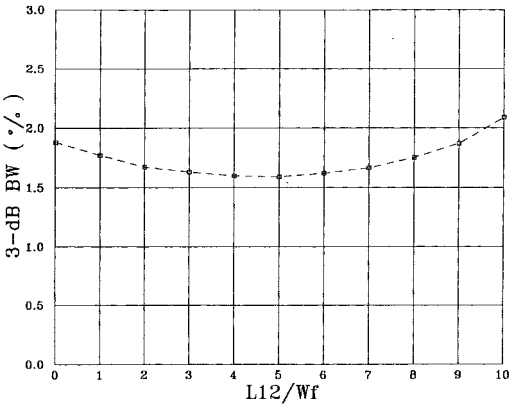

Fig. 10. Simulated variation of the percentage 3-dB bandwidth with the interstage coupling stub length L_{12}, as indicated in Fig. 6.

E. Comparison of a Hairpin-Line Filter and the Open-Loop Structure Presented in this Section

At first sight, the proposed open-loop structure seems like a hairpin-line filter [2]. However, a hairpin line is a folded open-ended resonator, which is quite similar to the shape of a wicket. Since the two folded arms of a hairpin line are pretty close to each other, the hairpin line itself is more like a pair of edge-coupled lines with loop connection on one end and open ends on the other. Besides, the hairpin lines used for filter design are usually oriented up and down interchangeably. Therefore, the open-loop resonator, shown in Fig. 6, is quite different than a hairpin structure. Moreover, the typical 3-dB bandwidth achieved by hairpin lines for narrow-band filter design is about 5% [21], [22], which is relatively larger than the 2.8% 3-dB bandwidth obtained using the open-loop filter proposed in this section.

The new bandpass filter in Fig. 6 has proven to be compact and capable of providing very narrow bandwidth. However, its attenuation slopes are not as steep as those in a dual-mode elliptic-function ring resonator in which two dips outside the passband help make the attenuation slopes sharper [4]–[12]. In Section IV, it will be shown that the filter configuration presented in this section can be modified to fulfill this elliptic filtering function while preserving the features of narrow 3-dB bandwidth and compact size.

IV. A New Elliptic-Function Narrow-Band Bandpass Filter Using Open-Loop Resonators With Coupled and Crossing Lines

A. Formation of Two Deep Notches Outside the Passband

It is well known that an elliptic function bandpass filter which features two notches outside its passband offers steeper rolling skirts and, hence, better stopband rejection. By simply connecting an additional crossing line between the middle points of the two identical open-loop resonators in Fig. 6, a novel compact elliptic-function narrow-band bandpass filter can be created, and is shown in Fig. 11. In addition to the coupled line laid along the open ends of the open-loop resonators where the maximum electric field intensity exists, this crossing line is intended to provide another type of

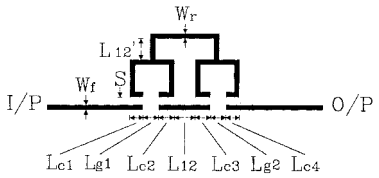

Fig. 11. The novel compact elliptic narrow-band bandpass filter using open-loop resonators together with coupled and crossing lines proposed in this paper.

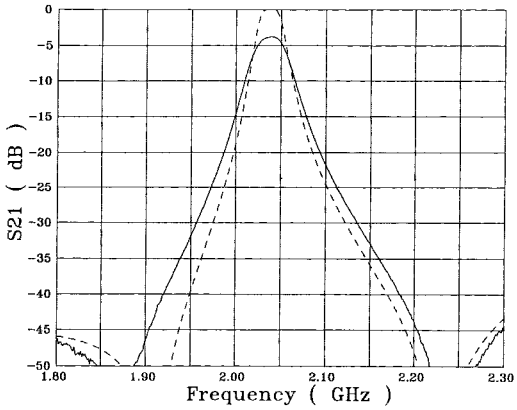

Fig. 12. Theoretical (dashed line) and measured (solid line) frequency responses of the novel compact filter, as depicted in Fig. 11.

perturbation at the current maxima in the resonators. Through dual-path interaction of electromagnetic (EM) waves, it is shown in Section IV-B that two deep notches in the stopband can be produced accordingly.

B. Simulated Performance and Measured Results

For convenience of comparison, the fabricated filter uses the same circuit parameters as those given in Section III-B, except for $L_{12}{}'$ which is set equal to $3W_f$ for the reasons described later. As shown in Fig. 12, the computer simulation and measurements show that two deep notches in the stopband can be created with improved stopband characteristics. Inspection of Fig. 12 indicates that the 3-dB bandwidth centered at 2.039 GHz is just 1.96%, which obviously makes this structure quite attractive for PCS applications. In addition, the circuit size is quite small (2.5 $\times$ 1.5 cm).

Although the insertion loss is measured 3.7 dB, it can easily be increased to 2.6 dB by just placing two 2 mm $\times$ 2 mm dielectric overlays of the same substrate as the circuit board over the interstage coupling gaps. The comparison of the measured frequency responses of the new elliptic-function narrow-band bandpass filter in Fig. 11, with and without the dielectric overlays, is shown in Fig. 13. The 3-dB bandwidth is increased slightly from 1.96% to only 2.21% by the overlays.

In general, this novel configuration for bandpass filter realization is able to provide a 2% 3-dB bandwidth in the passband and sharper rolling skirts for stopband rejection. Since all the ring linewidths are set the same as those for the input and output feeding lines, further improvement in performance can be made by optimizing these widths.

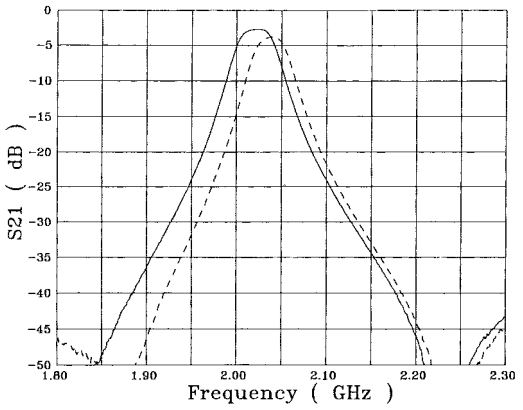

Fig. 13. Comparison of the measured frequency responses of the novel filter in Fig. 11 with (solid line) and without (dashed line) dielectric overlays of relative dielectric constant = 10.5 and thickness = 50 mil placed on both the interstage coupling gaps.

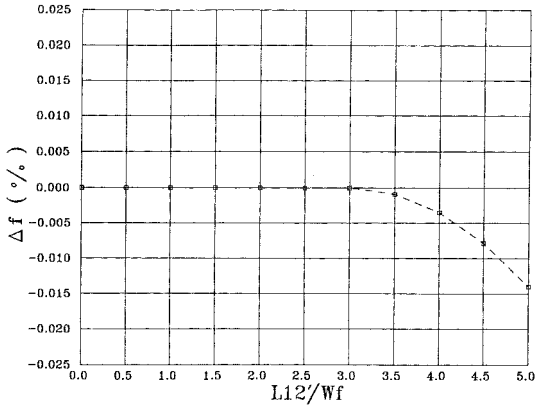

Fig. 14. Simulated percentage center-frequency drift $\Delta f = [f_0(L_{12}{}') - f_0(L_{12}{}' = 3W_f)]/f_0(L_{12}{}' = 3W_f) \times 100\%$ versus the interstage crossing stub length $L_{12}{}'$, as indicated in Fig. 11.

C. Effects of the Crossing Line on Center Frequency and Bandwidth

Similar to the auxiliary interstage coupling stub, the crossing line in Fig. 11 is used mainly to provide another coupling path and should be kept as short as possible. The effects of this length on the central resonant frequency and the passband bandwidth have been studied. Let the center frequency f_0 with $L_{12}{}' = 3W_f$ be the reference value, the center frequency drift Δf is defined as

$$\Delta f = [f_0(L_{12}{}') - f_0(L_{12}{}' = 3W_f)]/f_0(L_{12}{}' = 3W_f) \times 100\%. \tag{7}$$

As indicated in Fig. 11, $L_{12}{}'$ is a segment of the coupling line that joins the current maximum of each open-loop resonator. It should be long enough to avoid possible edge coupling between this crossing line and the resonators. On the other hand, it has to be made as short as possible to keep the circuit compact. Shown in Figs. 14 and 15 are the simulated center frequency shift and 3-dB bandwidth variations with the segment $L_{12}{}'$ defined in Fig. 11. It is apparent that the effects of this segment on the center frequency and bandwidth are negligible as long as its length is less than three times the

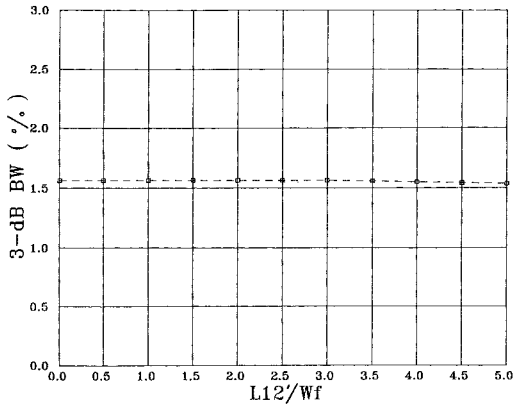

Fig. 15. Simulated variation of the percentage 3-dB bandwidth with the interstage crossing stub length $L_{12}{}'$, as indicated in Fig. 11.

transmission linewidth. This is the reason why $L_{12}{}' = 3W_f$ has been selected.

Before concluding this subsection, it is worth mentioning one more point. Due to the addition of the interstage crossing line in the bandpass filter of Fig. 11, another open-end resonator that takes the longest path has actually been created. From computer simulation, the first harmonic of this extra open end will appear in the upper stopband if the segment $L_{12}{}'$, defined in Fig. 11, is made much longer than suggested. In case it appears near the passband, the spurline bandstop filters, which are space-saving and capable of offering 20% bandwidth, can be utilized to eliminate this spurious response [23].

D. Comparison of a Standard Dual-Mode Ring Structure and the Elliptic-Function Open-Loop Filter Described in this Section

Since the circumference of a standard ring is one wavelength and the open-loop resonator used in this paper is a half-wave long, the area occupied by each open-loop resonator is about one-fourth that of a standard ring. In many applications where the available space of usable substrates is quite limited, size minimization of a filter structure is very important. Therefore, the open-loop resonator serves a good candidate for miniature filter design.

Usually a ring filter is directly coupled to the input and output feed lines and suffers from higher insertion loss due to insufficient end gap coupling. Hence, novel excitation schemes would have to be utilized to enhance the coupling strength [24]. However, the measured 3-dB bandwidth is also greatly increased when interdigital structures, for example, are used to bring down the impractically large insertion loss of a dual-mode ring filter [25].

Although each dual-mode ring filter can produce two poles in the passband, practical ring structures do suffer from tradeoff between low insertion loss and narrow passband bandwidth, unless active devices are incorporated for loss compensation [12]. As for the open-loop resonator depicted in Fig. 11, it is coupled to the feed lines by means of edge-coupled line sections, which can be flexibly adjusted to meet the specific insertion loss and bandwidth requirements.

V. Conclusions

A new type of planar filters using open-loop resonators together with coupled and crossing lines is proposed. It has been verified both theoretically and experimentally that this novel configuration can give a 2% 3-dB bandwidth and elliptic-function filter characteristics featuring two steep notches outside its passband. Moreover, the filter is very compact in size. These characteristics make this narrow-band bandpass filter quite useful for applications in today's PCS's.

If the entire filter could be simplified to a cascade of building blocks whose equivalent circuit models may be derived or reasonably approximated, then the standard filter theory can be applied for elliptic filter design with arbitrary positioning of the reflection zeros in the passband and transmission zeros in the stopband [2]. Otherwise, experimental design curves or EM full-wave simulators would have to be resorted to [13]. Since study on the equivalent circuit modeling for planar filters using either standard dual-mode rings or parallel-coupled open-loop resonators has not reached sufficient maturity, further research and development would need to be done on this subject.

Acknowledgment

The authors would like to thank M.-Y. Li for his exceptional technical assistance. Special gratitude is also extended to H. Tehrani and the anonymous reviewers for their helpful comments and suggestions that have made this paper more understandable.

References

[1] G. L. Matthaei, L. Young, and E. M. T. Jones, *Microwave Filters, Impedance-Matching Networks, and Coupling Structures.* New York: McGraw-Hill, 1964.

[2] J. A. G. Malherbe, *Microwave Transmission Line Filters.* Norwood, MA: Artech House, 1979.

[3] R. Levy and S. B Cohn, "A history of microwave filter research, design, and development," *IEEE Trans. Microwave Theory Tech.*, vol. MTT-32, pp. 1055–1067, Sept. 1984.

[4] M. Guglielmi and G. Gatti, "Experimental investigation of dual-mode microstrip ring resonator," in *Proc. 20th European Microwave Conf.*, Budapest, Hungary, Sept. 10–13, 1990, pp. 901–909.

[5] J. A. Curtis and S. J. Fiedziuszko, "Multi-layered planar filters based on aperture coupled, dual mode microstrip or stripline resonators," in *IEEE MTT-S Int. Microwave Symp. Dig.*, Albuquerque, NM, June 1–5, 1992, pp. 1203–1206.

[6] J. S. Hong and M. J. Lancaster, "Bandpass characteristics of new dual-mode microstrip square loop resonators," *Electron. Lett.*, vol. 31, no. 11, pp. 891–892, May 1995.

[7] ——, "Realization of quasielliptic function filter using dual-mode microstrip square loop resonators," *Electron. Lett.*, vol. 31, no. 24, pp. 2085–2086, Nov. 1995.

[8] ——, "Microstrip bandpass filter using degenerate modes of a novel meander loop resonator," *IEEE Microwave Guided Wave Lett.*, vol. 5, pp. 371–372, Nov. 1995.

[9] J. A. Curtis and S. J. Fiedziuszko, "Miniature dual mode microstrip filters," in *IEEE MTT-S Int. Microwave Symp. Dig.*, Boston, MA, June 10–14, 1991, pp. 443–446.

[10] R. R. Mansour, "Design of superconductive multiplexers using single-mode and dual-mode filters," *IEEE Trans. Microwave Theory Tech.*, vol. 42, pp. 1411–1418, July 1994.

[11] S. J. Fiedziuszko, J. A. Curtis, S. C. Holme, and R. S. Kwok, "Low loss multiplexers with planar dual mode HTS resonators," *IEEE Trans. Microwave Theory Tech.*, vol. 44, pp. 1248–1257, July 1996.

[12] U. Karacaoglu, I. D. Robertson, and M. Guglielmi, "A dual-mode ring resonator filter with active devices for loss compensation," in *IEEE MTT-S Int. Microwave Symp. Dig.*, Atlanta, GA, June 14–18, 1993, pp. 189–192.

[13] J. S. Hong and M. J. Lancaster, "Couplings of microstrip square open-loop resonators for cross-coupled planar microwave filters," *IEEE Trans. Microwave Theory Tech.*, vol. 44, pp. 2099–2108, Dec. 1996.
[14] M. Makimoto and M. Sagawa, "Varactor tuned bandpass filters using microstrip-line ring resonators," in *IEEE MTT-S Int. Microwave Symp. Dig.*, Baltimore, MD, June 2–4, 1986, pp. 411–414.
[15] K. Chang, *Microwave Ring Circuits and Antennas.* New York: Wiley, 1996.
[16] R. Crampagne and G. Khoo, "Synthesis of certain transmission lines employed in microwave integrated circuits," *IEEE Trans. Microwave Theory Tech.*, vol. MTT-25, pp. 440–442, May 1977.
[17] M. Abramowitz and I. A. Stegun, *Handbook of Mathematical Functions.* New York: Dover, 1964, ch. 17, pp. 590–592.
[18] K. C. Gupta, R. Garg, I. Bahl, and P. Bhartia, *Microstrip Lines and Slotlines*, 2nd Ed. Norwood, MA: Artech House, 1996, sec. 3.4.2, pp. 183–189.
[19] K. Chang and J. L. Klein, "Dielectrically shielded microstrip (DSM) lines," *Electron. Lett*., vol. 23, no. 10, pp. 535–537, May 1987.
[20] J. L. Klein and K. Chang, "Optimum dielectric overlay thickness for equal even- and odd-mode phase velocities in coupled microstrip circuits," *Electron. Lett.*, vol. 26, no. 5, pp. 274–276, Mar. 1990.
[21] E. G. Cristal and S. Frankel, "Hair-line and hybrid hairpin-line/half-wave parallel-coupled-line filters," *IEEE Trans. Microwave Theory Tech.*, vol. MTT-20, pp. 719–728, Nov. 1972
[22] U. H. Gysel, "New theory and design for hair-line filters," *IEEE Trans. Microwave Theory Tech.*, vol. MTT-22, pp. 523–531, May 1974.
[23] C. Nguyen and K. Chang, "Analysis and design of spurline bandstop filters," *IEEE MTT-S Microwave Symp. Dig.*, St. Louis, MO, June 1985, pp. 445–448.
[24] G. K. Gopalakrishnan and K. Chang, "Novel excitation schemes for the microstrip ring resonator with lower insertion loss," *Electron. Lett.*, vol. 30, no. 2, pp. 148–149, Jan. 1994.
[25] U. Karacaoglu, D. Sanchez-Hernandez, I. D. Robertson, and M. Guglielmi, "Harmonic suppression in microstrip dual-mode ring-resonator bandpass filters," in *IEEE MTT-S Microwave Symp. Dig.*, San Francisco, CA, June 17–21, 1996, pp. 1635–1638.

Cheng-Cheh Yu (S'91–M'91) was born on January 1, 1964, in Taipei, Taiwan, R.O.C. He received the five-year-program diploma degree in electrical engineering from the National Taipei Institute of Technology, Taipei, Taiwan, R.O.C., in 1984, and the M.S. and Ph.D. degrees in electrical engineering from the National Taiwan University, Taipei, Taiwan, R.O.C., in 1988 and 1991, respectively.

From 1991 to 1992, he worked for the Telecommunication Ministry, Taiwan, R.O.C., as an Associate Researcher. He then joined the Department of Electronic Engineering, National Taipei University of Technology, where he was the Director of the Electrooptics Research and Development Center (1994–1996) and was promoted to Full Professor in 1997. In 1996, he was invited to Texas A&M University, as a Visiting Scholar, and conducted his research on narrow-band planar filter design. His professional interests include advanced EM theory, wave-guiding structures, multilayer planar transmission lines, microwave circuits, interconnects and packaging, antenna analysis/design, advanced computational EM's, passive/active RF filter designs, and electronic communication techniques.

Dr. Yu is a member of the American Radio Relay League (ARRL), and a life member of the Institute of the Chinese Electrical Engineers (CIEE). He holds the R.O.C. Certificate of National Advanced Official Examination (1985). In 1996, he received the first position in the National Examination for Overseas Study sponsored by the R.O.C. Educational Ministry. He has also received research awards from the National Science Council (1993) and the National Taipei Institute of Technology (1996 and 1998). In 1995, he was elected as one of the top 100 outstanding youths in Taiwan, R.O.C., and received a Special Achievement Award from the National Taipei University of Technology.

Kai Chang (S'75–M'76–SM'85–F'91) received the B.S.E.E. degree from the National Taiwan University, Taipei, Taiwan, R.O.C., in 1970, the M.S. degree from the State University of New York at Stony Brook, in 1972, and Ph.D. degree from the University of Michigan at Ann Arbor, in 1976.

From 1972 to 1976, he worked as a Research Assistant for the Microwave Solid-State Circuits Group, Cooley Electronics Laboratory, University of Michigan at Ann Arbor. From 1976 to 1978, he was with Shared Applications, Inc., Ann Arbor, MI, where he worked in computer simulation of microwave circuits and microwave tubes. From 1978 to 1981, he worked for the Electron Dynamics Division, Hughes Aircraft Company, Torrance, CA, where he was involved in the research and development of millimeter-wave solid-state devices and circuits, power combiners, oscillators, and transmitters. From 1981 to 1985, he worked as a Section Head for the TRW Electronics and Defense, Redondo Beach, CA, developing state-of-the-art millimeter-wave integrated circuits and subsystems including mixers, voltage-controlled oscillators (VCO's), transmitters, amplifiers, modulators, upconverters, switches, multipliers, receivers, and transmitters. He then joined the Electrical Engineering Department, Texas A&M University as an Associate Professor and was promoted to Full Professor in 1988. In 1990, he was appointed E-Systems Endowed Professor of electrical engineering. He has authored and co-authored *Microwave Solid-State Circuits and Applications* (New York: Wiley, 1994), *Microwave Ring Circuits and Antennas* (New York: Wiley, 1996), *Integrated Active Antennas and Spatial Power Combining*, (New York: Wiley, 1996), and has served as editor for the four-volume *Handbook of Microwave and Optical Components* (New York: Wiley, 1989, 1990), the Wiley Microwave and Optical Engineering Book Series, and *Microwave and Optical Technology Letters*. He has also published over 250 technical papers and several book chapters in the areas of microwave and millimeter-wave devices, circuits, and antennas. His current interests are in microwave and millimeter-wave devices and circuits, microwave integrated circuits, integrated antennas, wide-band and active antennas, phased arrays, power transmission, and microwave optical interactions.

Dr. Chang received the Special Achievement Award from TRW and the Halliburton Professor Award (1988), the Distinguished Teaching Award (1989), the Distinguished Research Award (1992), and the TEES Fellow Award (1996) from Texas A&M University.